

COMBINATION OF FUZZY AND "CRISP" PRINCIPLES IN MODERN MUTIVARIABLE ROBUST FLIGHT CONTROL

Introduction

In the last years, the problem of the flight control system robustness became a challenge for designers. Several methods have been proposed in the area [1]. In the present paper the combination of the fuzzy inference system and the traditional control is investigated in order to achieve the aforementioned objective. The complexity of the task brought us to divide the design procedure into two stages. At the first stage the inner loop controller is designed based on the crisp controller, the second stage is devoted to the design of the outer loop controller based on the fuzzy system. In the design of flight control law one should care about many problems, especially in the area of unmanned aerial vehicles (UAV), due to the expensive cost of the on-board computers and navigation sensors as well as to the weight, cost and power consumption of the UAV, which should be reduced to the minimum. For these reasons the control law should be simple enough and should respond to the expected performances and robustness requirements of the flight control. In order to reduce the navigation sensors and the weight and cost of the UAV, in this paper, the optimal controller is designed for the inner loop based on the separation theorem [9]. The state estimator is used to restore the unavailable measurements which could be contaminated by noises, in the next step a state feedback control law is designed for the filtered states based on the linear quadratic regulation.

However, during the flight, the UAV is vulnerable towards the changeable of atmospheric conditions and parameters of the plant model. Hence, the designed control law may not keep the predefined objectives of robustness and performances. The H_2/H_∞ - robust optimization is used to seek the trade off between the performances and robustness of the inner loop controller [7, 8].

In the second stage the fuzzy system is used to design the outer loop control law. The fuzzy controller used in this report is inspired from the well known conventional adaptive controller called model ref-

erence adaptive controller (MRAC) [12]. Such controllers have the learning ability from a reference model which approximates the dynamic of flight. The fuzzy controller is used to hold the altitude of the UAV [1]. The design of fuzzy controller is based on ad-hoc method and on the expert's knowledge, by this fact the rule base of the controller may not be consistent and/or the expert could omit some uncertainties which can occur during the flight. For this reason, the fuzzy controller should update or adjust its rule base constantly to overcome the aforementioned problems. To do so, the dynamic of the controlled model is approximated in the reference model and the fuzzy controller learns from it to synthesize and/or adjust its knowledge base during the flight, this method is called Model Reference Teaming Control (FMRTC) [14].

The choice of such combination of 'crisp' and fuzzy control can be justified by the following reasons: the order of the mathematical model is very high, and for satisfying of stability and performance requirements the controller must use information from many sensors. It in turn requires very large amount of inference rules and the knowledge base of the fuzzy controller would be unfeasible. In case of combined system fuzzy controller could be essentially simplified: two or even one input would be enough.

Inner loop control law

The inner loop controller is designed using the separation theorem [3, 9] to stabilize the true airspeed V_t and the pitch angle. The state space model of the controlled plant is given by the following matrices $[A, B, C, D, G]$, where $A \in \mathbb{R}^{n \times n}$, $B \in \mathbb{R}^{n \times q}$, $C \in \mathbb{R}^{p \times n}$, $D \in \mathbb{R}^{p \times q}$, $G \in \mathbb{R}^{n \times 1}$, and is given by:

$$\begin{aligned} \dot{X} &= AX + BU + Gw \\ Y &= CX + DU + v \end{aligned} \quad (1)$$

The vector w represents the process disturbances (wind turbulence), described by the outputs of the Dryden filter, v is the sensors noises. In order to apply the separation theorem it would be necessary to include the model of the wind turbulence. In this paper it is given by the Dryden filter [7]. Let the quadruple matrices $[A_{dr}, B_{dr}, C_{dr}, D_{dr}]$ represents the state space model of the forming filter, where $A_{dr} \in \mathbb{R}^{r \times r}$, $B_{dr} \in \mathbb{R}^{r \times 2}$, $C_{dr} \in \mathbb{R}^{1 \times r}$, $D_{dr} \in \mathbb{R}^{1 \times r}$, this task is performed using series

connection of the mentioned filter and the state space model of the UAV, the extended state space model of the overall model is described in the following:

$$\left[\begin{array}{c|c} \mathbf{A}_{\text{ex}} & \mathbf{B}_{\text{ex}} \\ \hline \mathbf{C}_{\text{ex}} & \mathbf{D}_{\text{ex}} \end{array} \right] = \left[\begin{array}{cc|cc} \mathbf{A} & \mathbf{GC}_{\text{dr}} & \mathbf{B} & \mathbf{GB}_{\text{dr}} \\ \mathbf{0}_{r \times n} & \mathbf{A}_{\text{dr}} & \mathbf{0}_{r \times q} & \mathbf{B}_{\text{dr}} \\ \hline \mathbf{C} & \mathbf{0}_{p \times r} & \mathbf{D} & \mathbf{0}_{p \times 2} \end{array} \right] \quad (2)$$

The state space model represented in (2) is 'contaminated' by noises and some states are not available for measurement, which justifies the use of Kalman filter to restore the full measurements, after reconstructing the full states an optimal deterministic controller- state feedback is designed [9]. The optimal Kalman filter is defined as:

$$\begin{aligned} \dot{\tilde{\mathbf{X}}} &= \mathbf{A}_{\text{ex}} \tilde{\mathbf{X}}_{\text{ex}} + \mathbf{B}_{\text{ex}} \mathbf{U} + \mathbf{L}(\mathbf{Y} - \mathbf{C}_{\text{ex}} \tilde{\mathbf{X}}_{\text{ex}} - \mathbf{D}_{\text{ex}} \mathbf{U}) \\ \begin{bmatrix} \tilde{\mathbf{Y}} \\ \tilde{\mathbf{X}} \end{bmatrix} &= \begin{bmatrix} \mathbf{C}_{\text{ex}} \\ \mathbf{I} \end{bmatrix} \tilde{\mathbf{X}}_{\text{ex}} + \begin{bmatrix} \mathbf{D}_{\text{ex}} \\ \mathbf{0} \end{bmatrix} \mathbf{U} \end{aligned} \quad (3)$$

where L is the Kalman gain matrix given by the following expression:

$$\mathbf{L} = \mathbf{P} \mathbf{C}_{\text{ex}}^T \mathbf{R}_N^{-1} \quad (4)$$

and P is solution to the following *Algebraic Riccati Equation (ARE)*:

$$\mathbf{A}_{\text{ex}} \mathbf{P} + \mathbf{P} \mathbf{A}_{\text{ex}}^T + \mathbf{B}_{\text{ex}} \mathbf{Q}_N \mathbf{B}_{\text{ex}}^T - \mathbf{P} \mathbf{C}_{\text{ex}}^T \mathbf{R}_N^{-1} \mathbf{C}_{\text{ex}} \mathbf{P} = \mathbf{0} \quad (5)$$

where \mathbf{Q}_N and \mathbf{R}_N are the covariance matrices associated to the measurement and process noises respectively. In accordance with separation theorem [5] state feedback K is given in the following expression:

$$\mathbf{K} = \mathbf{R}^{-1} \mathbf{B}_{\text{ex}}^T \mathbf{S} \quad (6)$$

where S is the unique positive definite matrix of the *ARE* associated to the optimal feedback problem:

$$\mathbf{A}_{\text{ex}}^T \mathbf{S} + \mathbf{S} \mathbf{A}_{\text{ex}} - \mathbf{S} \mathbf{B}_{\text{ex}} \mathbf{R}^{-1} \mathbf{B}_{\text{ex}}^T \mathbf{S} + \mathbf{Q} = \mathbf{0} \quad (7)$$

and the optimal control law minimizing the LQR performance index, is given as:

$$\mathbf{U} = -\mathbf{K} \tilde{\mathbf{X}}_{\text{ex}} \quad (8)$$

In accordance with separation theorem [5] crisp controller consists of combination of Kalman filter (3) and state feedback (8), and the state space model of the inner loop crisp controller is given in the following:

$$\begin{bmatrix} \dot{X} \\ \dot{\tilde{X}} \end{bmatrix} = \begin{bmatrix} A_{ex} & -B_{ex}K \\ LC_{ex} & A_{ex} - LC_{ex} - B_{ex}K \end{bmatrix} \begin{bmatrix} X \\ \tilde{X} \end{bmatrix} \quad (9)$$

At this stage the crisp controller is synthesized and in the next paragraph we the trade off between the performances and the robustness is studied.

Parameterization and robustization of the inner loop controller

The most wanted and expected property of flight controller law is the robustness. Throughout the flight, the UAV is subject to the disturbances, which could be external and/or internal, structural and/or unstructured and produce certain deviation from the nominal behavior to the perturbed one. This deviation could be represented by other model called parametrically perturbed model. The main idea of the H_2/H_∞ - robust optimization is to provide the same level of performances for the nominal and perturbed models with the same controller designed to the nominal. Many methods are proposed in the area of robust flight control [6, 7]. The method used in this paper is based on using the H_2 - norm of the sensitivity function to estimate the performances of the control system, H_∞ - norm of the complementary sensitivity function is used to estimate the robustness [16].

The nonlinear model of the plant is 'linearized' at N operating conditions inside the flying envelope, after linearization N linear models are found; the control law is designed for one linear model and should keep the same performances and robustness for all N models. To do so the compromise should be found between the robustness and the performances for all operating conditions.

The sensitivity and complementary sensitivity functions are computed for the N closed loop systems. It can be seen that these functions are depending on Kalman gain matrix L and state feedback K , hence these parameters constitute the variables of the optimization procedure.

A composite performance index is formed from the estimation of the performances and the robustness for the N models based on the H_2/H_∞ - norms computed for the different transfer functions [8, 11] of the block diagram depicted in the Figure 1.

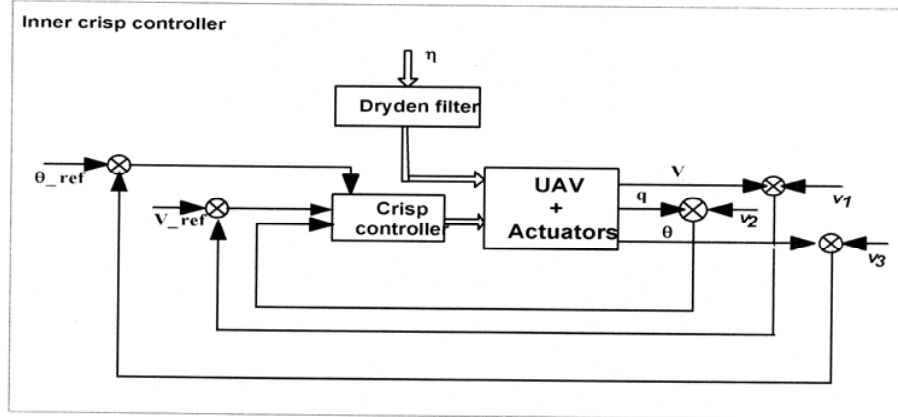


Figure 1-The inner loop controller

In the following expression the performance index to be optimized is given [6]:

$$J(K, L) = \lambda_{dn} \|S\|_2^{dn} + \lambda_{sn} \|S\|_2^{sn} + \lambda_{\infty n} \|T\|_{\infty}^n + \sum_{k=1}^{N-1} \lambda_{dpk} \left(\|S\|_2^{dpk} \right) + \sum_{k=1}^{N-1} \lambda_{spk} \left(\|S\|_2^{spk} \right) + \sum_{k=1}^{N-1} \lambda_{\infty pk} \left(\|T\|_{\infty}^{pk} \right) \quad (10)$$

where $\|S\|_2^{dn}$ defines the H_2 -norm of the nominal model in deterministic case, $\sum_{k=1}^{N-1} \|S\|_2^{dpk}$ stand for summation of the H_2 - norms of $(N - 1)$ perturbed models. $\|T\|_{\infty}^n$ is the H_{∞} -norm and gives the estimation of the robustness of the nominal controlled plant, $\sum_{k=1}^{N-1} \|T\|_{\infty}^{pk}$ computes the summation of the H_{∞} norm for all $(N - 1)$ parametrically disturbed plants. $\|S\|_2^{sn}$ defines the performances of the nominal stochastic model, same summation of the H_2 -norm defined for all perturbed models with the expression $\sum_{k=1}^{N-1} \|S\|_2^{spk}$. The LaGrange factors λ_{dn} , λ_{sn} , λ_{dpk} , λ_{spk} , $\lambda_{\infty n}$, $\lambda_{\infty pk}$ define the weights of each term in the cost function.

Outer loop control law

The functional diagram of the fuzzy controller used in this study is depicted in the Figure 2.

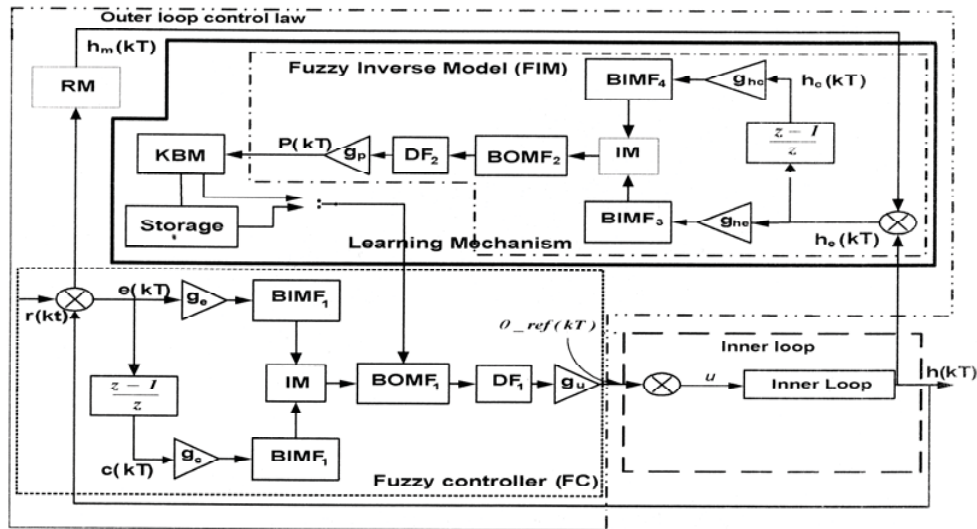


Figure 2 - Block diagram of FMRLC

It has four main parts [14]: the inner loop control model, which is described in the previous chapter; the fuzzy controller (FC), the reference model (RM) and the learning mechanism, which is divided into two parts fuzzy inverse model (FIM) and knowledge base modifier (KBM). The goal of this method is to synthesize fuzzy controller and to adjust its membership functions in order to withstand to the action of parametric disturbances in the controlled plant. The different parts of the scheme are explained in the next section.

Fuzzy control of the altitude

The input to the FC is the error $e(kT)$ between the reference altitude $r(kT)$ and altitude output $h(kT)$ of UAV and the second input is the change rate of this error $c(kT)$. The FC output is the $\theta_{ref}(kT)$ and represents the reference input to the inner Attitude Control Loop (ACL).

$$e(kT) = r(kT) - h(kT) \quad (11)$$

$$c(kT) = \frac{e(kT) - e(kT - T)}{T} \quad (12)$$

The universes of discourse of the membership function of the FC are normalized to be between $[-1 \ 1]$ by the mean of scaling factors g_e , g_c and g_u for error $e(kT)$, $c(kT)$ and $\theta_{ref}(kT)$ universe of discourse, respectively. The inference mechanism (IM) is Mamdani type, and it can be expressed in the form of IF-THEN, the input membership functions are implemented in $BIMF_1$ for the altitude error and $BIMF_2$ for the change in altitude error, the output membership functions are given in the $BOMF_1$. The defuzzification method used in our case is the Center

Of Gravity (COG) and implemented in the block DF₁, and the control action is given by the following expression [15]:

$$\theta_{ref_n^*}(kT) = \frac{\sum_{k=1}^l \hat{A}_n^k(kT) \hat{c}_n(kT)}{\sum_{k=1}^l \hat{A}_n^k(kT)}$$

$$\theta_{ref_n^*}(kT) = \frac{\sum_{k=1}^l A_n^k(kT) c_n(kT)}{\sum_{k=1}^l A_n^k(kT)} \quad (13)$$

Where $A_n^1(kT)$ and $c_n(kT)$ are the areas and the centers of areas, associated with the resulted fuzzy set from the aggregated fuzzy set [15].

The reference model (RM)

The reference model generates the desired performance of the overall process. In general, the reference model may be any type of dynamical system. The performance of the overall system is computed with respect to its output $h_m(kT)$ by generating an error signal,

$$h_e(kT) = h_m(kT) - h(kT) \quad (14)$$

In our case the reference model approximated with second order model with settling time 30 seconds and without overshoot.

The learning mechanism [14]

As previously mentioned, the learning mechanism performs the function of modifying the knowledge base (membership functions) of the direct fuzzy controller so, that the closed loop system behaves like the reference model. These knowledge base modifications are made on the basis of observing data from the controlled process, the reference model and the fuzzy controller. In accordance with Fig. 2 the learning mechanism consists of two parts: a fuzzy inverse model (FIM) and a knowledge base modifier (KBM). FIM performs the function of mapping the error $h_e(kT)$ and the change of error $h_c(kT)$, to the changes of the FC output membership function's parameters $p = [p_1, \dots, p_r]^T$ in BOMF₁, which are necessary to force $h_e(kT)$ to zero. These parameters are the shifts of positions of the output membership function's centers. KBM performs the function of modifying the fuzzy controller's knowledge base to perform

the needed change in the process inputs. More details of this process are discussed next. The fuzzy inverse model uses the same inference mechanism as the fuzzy controller (FC). It is not necessary for fuzzy control to accurately characterize the inverse dynamics; only approximate representation is needed [14]. FIM simply maps $h_e(kT)$ and $h_c(kT)$ to the necessary changes in the plant inputs, that is why it is called "fuzzy inverse model". Hence, FIM is used to characterize how to change the plant inputs to force the plant output $h(kT)$ to follow $h_m(kT)$ as close as possible. Likewise to the fuzzy controller, the FIM shown in Fig. 2 contains normalizing scaling factors, namely g_{he} , g_{hc} and g_p for each universe of discourse. Selection of the normalizing gains can impact the overall performance of the system. The knowledge base for the fuzzy inverse model is generated from fuzzy rules of the form:

$$\text{IF } \tilde{h}_e \text{ is } H_e^j \text{ AND } \tilde{h}_c \text{ is } H_c^k \text{ THEN } \tilde{p} \text{ is } P^{j,k}$$

$P^{j,k}(kT)$ is the necessary variation of the position of the membership function's center, decreasing $h_e(kT)$.

The knowledge base modifier (KBM)

KBM performs the function of modifying the FC rule base to achieve better performance. Given the information about the necessary changes in the plant input, which are represented by $p(kT)$, to force the error $h_e(kT)$ to zero, the knowledge base modifier change the FC rule-base so that the previously computed control action $\theta_{\text{ref}}(kT - T)$ would be modified at the next step as follows: $\theta_{\text{ref}}(kT - T) + p(kT)$. By modifying the fuzzy controller's knowledge base, we may force the fuzzy controller to produce a desired output, which we should put in at time $kT - T$ to make $h_e(kT)$ smaller. Then the next time we get similar values for the error and change in error, the input to the plant will be one that will reduce the error between the reference model and the plant output.

Assume that we use symmetric output membership function for the fuzzy controller, and let b_1 denote the center of the membership function associated with $\tilde{\theta}_1_{\text{ref}}$. Knowledge base modification is performed by shifting centers b_1 of the membership function of the output linguistic value $\tilde{\theta}_1_{\text{ref}}$, which are associated with the fuzzy controller rules

that contributed to previous control action $\theta_{\text{ref}}(kT - T)$. This is two-step process:

1. Find all FC rules, which satisfy the following condition:

$$\tau_k(e(kT - T), c(kT - T)) > 0 \quad (15)$$

$k = (1, 1)$, τ_k defines the set of the Degrees of Firing (DOF) of rules at time $kT - T$, also called "active set".

2. Let b_l denote the center of l^{th} output membership function at time kT . For all rules in the active set, use $b_l(kT) = b_l(kT - T) + p_l(kT)$ to modify the output membership function centers. Rules that are not in the active set do not have their membership function modified. KBM includes also the storage (see Fig. 2), which preserves the results of tuning of membership functions, in order to be used when the output of the FC at time kT is the same at $kT-1$.

Design and implementation of FMLRC [14]

The total design procedure for the FMRLC, which is used in combination with "crisp" feedback, involves the following steps:

- The specification of a direct fuzzy controller with consequent membership functions that can be tuned. This fuzzy controller can be chosen via conventional (heuristic) fuzzy control design techniques for the nominal plant.

- Specifying the reference model of control system, which characterizes the desired system performance.

- Specifying the fuzzy inverse model, which characterizes how the inputs to the plant should be changed so, that the desired performance is achieved.

- Selection of the normalizing gains for the fuzzy controller and the fuzzy inverse model.

So far as the selection of the normalizing gains for both the fuzzy controller and the fuzzy inverse model can impact the overall performance, it is necessary to provide a procedure for choosing these parameters. Due to physical constraints for a given system, the range of values for the process inputs and outputs is generally known from a qualitative analysis of the process especially, when the crisp prototype of system is determined via some known procedure of control synthesis. As a result, we can determine the range of values or the universe of discourse for

$e(kT)$, $u(kT)$, $h_e(kT)$ and $p(kT)$. Consequently, g_e , g_c , g_u , g_{he} and g_p are chosen so that the appropriate universes of discourse are mapped to $[-1, 1]$. They could be determined on the basis of the "crisp" prototype by iteratively applying inputs to $r(kT)$, observing $c(kT)$, and finding scaling factors to map the universes of discourse to the interval $[-1, 1]$.

Case study

In this paper the longitudinal channel of unmanned aerial vehicle (UAV) Aerosonde in altitude and true airspeed stabilization mod is used as a case study. The full nonlinear model of this UAV is represented in [2]. The state space vector is $\bar{X} = [u \ w \ q \ \theta \ h \ \Omega]$, u , w - horizontal and vertical velocity component, respectively; q - pitch rate, θ - pitch angle, h - altitude and Ω - engine spin (r.p.m.). The control vector is given by $\bar{U} = [\delta_e \ \delta_{lh}]$, where δ_e - elevator angle deflection, δ_{lh} - thrust control (engine throttle deflection). The range of the uncertainty is made for the true airspeed, which is given by the following expression $V = \sqrt{u^2 + v^2 + w^2}$, where v defines the lateral velocity component. We suppose that V changes in the interval $25 \leq V \leq 35 \frac{\text{m}}{\text{sec}}$, for the sake of simplicity and without loss of generality three ($N = 3$) models were defined in our study, the nominal model is taken at $V_n = 30 \text{ m/sec}$. The first perturbed is defined for $V_n = 25 \text{ m/sec}$ and for the second perturbed model is defined for $V_n = 35 \text{ m/sec}$. The next matrices give the respective states space models:

$$A_n = \begin{bmatrix} -0.293 & 0.38 & -0.55 & -9.78 & 0 & 0.01 \\ -0.55 & -5.36 & 30 & -0.18 & 0 & 0 \\ 0.33 & -5.63 & -6.19 & 0 & 0 & 0 \\ 0 & 0 & 1 & 0 & 0 & 0 \\ 0.01 & -1 & 0 & 30 & 0 & 0 \\ 41.53 & 0.78 & 0 & 0 & -0.63 & -3.85 \end{bmatrix};$$

$$B_n = \begin{bmatrix} -0.3 & 0 \\ -3.7 & 0 \\ -50 & 0 \\ 0 & 0 \\ 0 & 0 \\ 0 & 2664 \end{bmatrix} \quad (16)$$

$$A_{p1} = \begin{bmatrix} -0.24 & 0.53 & -1.19 & -9.80 & 0 & 0.01 \\ -0.56 & -4.47 & 25 & -0.47 & 0 & 0 \\ 0.43 & -4.48 & -5.15 & 0 & 0 & 0 \\ 0 & 0 & 1 & 0 & 0 & 0 \\ 0.04 & -1 & 0 & 25 & 0 & 0 \\ 35 & 1.68 & 0 & 0 & -0.03 & -3.23 \end{bmatrix};$$

$$B_{p1} = \begin{bmatrix} 0.35 & 0 \\ -2.54 & 0 \\ -35.21 & 0 \\ 0 & 0 \\ 0 & 0 \\ 0 & 390 \end{bmatrix} \quad (17)$$

$$A_{p2} = \begin{bmatrix} -0.35 & 0.28 & -0.05 & -9.82 & 0 & 0.01 \\ -0.55 & -6.25 & 35 & -0.01 & 0 & 0 \\ 0.28 & -6.43 & -7.21 & 0 & 0 & -0.01 \\ 0 & 0 & 1 & 0 & 0 & 0 \\ 0 & -1 & 0 & 35 & 0 & 0 \\ 48.5 & 0.08 & 0 & 0 & -0.78 & -4.43 \end{bmatrix};$$

$$B_{p2} = \begin{bmatrix} 0.5 & 0 \\ -5 & 0 \\ -68.2 & 0 \\ 0 & 0 \\ 0 & 0 \\ 0 & 3040.3 \end{bmatrix} \quad (18)$$

The models of actuators are connected to the model of the UAV in series and they are approximated by the first order model given in the following:

$$W_{\text{act}} = \frac{1}{\tau_{\text{act}}p + 1} \quad (19)$$

where $\tau_{\delta_{\text{act}}} = 0.25 \text{ sec}$ stand for the time constant of the actuator and the subscript $\tau_{\delta_{\text{act}}}$ can be either for elevator or throttle.

In our design only four state variables are measured: $\bar{X} = [u, q, \theta, h]$, so the observation matrix is given as follows:

$$C = \begin{bmatrix} [1 & 0_{3 \times 1}]^T & 0_{4 \times 1} & [0_{1 \times 4} & I_{3 \times 3} & 0_{3 \times 1}]^T \end{bmatrix}$$

where I represents the unity matrix with appropriate dimension. The state vector $\bar{X}_{\text{inner}} = [u, q, \theta]$ constitute the inner loop feedback, the state variable h is the injected to the fuzzy reference model learning control. As shown before, in order to apply the separation theorem a turbulence model represented by the Dryden filter [5, 6, 7], which has two inputs: horizontal and vertical wind gusts, the outputs are the longitudinal turbulent speed (u_g), vertical turbulent speed (w_g) and turbulent pitch rate (q_g).

State space of the Dryden filter is defined by the following matrices:

$$A_{\text{dr}} = \begin{bmatrix} -1/\lambda_u & 0 & 0 \\ 0 & -1/\lambda_w & 0 \\ 0 & -K/\lambda_q^2 & -1/\lambda_q \end{bmatrix}; B_{\text{dr}} = \begin{bmatrix} K_u/\lambda_u & 0 \\ 0 & K_w/\lambda_w \\ 0 & 0 \end{bmatrix};$$

$$C_{\text{dr}} = \begin{bmatrix} 1 & 0 & 0 \\ 0 & 1 & 0 \\ 0 & K_q/\lambda_q & 1 \end{bmatrix}$$

where the subscript w corresponds to vertical components and u for the longitudinal. In our case the Aerosonde flies at an altitude of $200m$, and in moderate turbulence. The parameters appearing in the state space of Dryden filter are given in the following [5, 6, 7]:

$$K_u = \sigma_u \sqrt{(2L_u/\pi V)}, \quad \lambda_u = L_u/V, \quad K_w = 2.2, \quad \lambda_w = 0.6, \quad K_q = 1/V,$$

$$\lambda_q = 4b/\pi V,$$

where b is the wing span of the Aerosonde $b = 2.9m$. The same parameters are defined for different models with different true airspeed V .

Simulation results

The simulation results are given in the following figures, the table 2 represents the H_2 -norms for the nominal model and the perturbed models in deterministic and stochastic cases, H_∞ -norm is also computed and is given in the table.

The covariance matrices of the process noises and measurement noises are equal to $R_n = \text{diag}([1.5 \quad 2])$, $Q_n = \text{diag}([0.5 \quad 0.1 \quad 0.004])$, respectively, they are defined by the accuracy of the sensors. The weighting matrices Q_r , R_r for the optimal deterministic performance are given as: $Q_r = \text{diag}([20 \quad 2 \quad 0.1 \quad 0.5 \quad 0.00013 \quad 0.1 \quad 0.1 \quad 0.1 \quad 0.1 \quad 0.1])$, $R_r = \text{diag}([1 \quad 1])$. Using the above models it is possible to define an extended model containing 10 states, so the Kalman filter is using 3 measured states to restore 10 ones. On the basis of separation theorem the restored states are controlled by the deterministic optimal controller and the gain matrix K in (6) is found as follows:

$$K = \begin{bmatrix} 0.576 & 0.022 & -1.373 & -6.838 & 0.001 & -0.337 & 0.424 & -0.679 & 5.058 & 0.253 \\ 3.514 & 0.313 & -0.174 & -9.961 & 0.011 & -0.316 & 0.118 & -0.100 & 0.267 & 3.027 \end{bmatrix}$$

For the sake of brevity in this paper the Kalman gain L , is not given.

The outer loop is used to hold the altitude at the reference value. Parameters of the fuzzy model reference learning control are set as follows; the input scaling factors of the fuzzy controller (FC), $g_e=0.004$ and $g_c=0.2$ for the altitude error and change in altitude error, respectively, the output of FC is normalized to the interval $[-1,1]$ with scaling $g_u=3$. The initial rule base of the fuzzy controller is shown in the Table 1.

The entries to this table are the centers of the output membership functions, which are chosen in this report to be symmetric triangular. The fuzzy inverse model (FIM) has the same structure with the following scaling factors $g_{he}=1/100$ for the error and $g_{hc}=8$ for the change rate of the error, the output membership functions are normalized with scaling $g_p=0.05$.

The reference model used in the simulation is a second order block represented in the following state space model

$$A_r = \begin{bmatrix} -1.1701 & -0.1701 \\ 0.5 & 0 \end{bmatrix}; B_r = \begin{bmatrix} 1 \\ 0 \end{bmatrix}; C_r = [0 \quad 0.1701]; D_r = 0.$$

Initial rule base of fuzzy controller (FC)

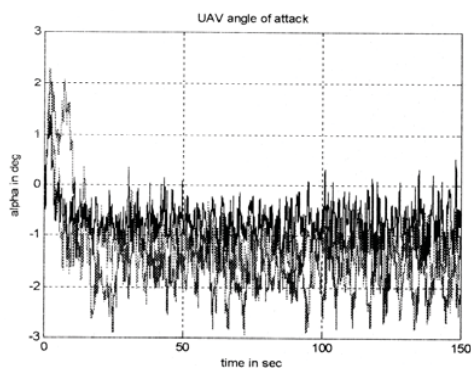
$U^{i,j}(kT)$	$e^i(kT)$												
		-1	-0.8	-0.6	-0.4	-0.2	0	0.2	0.4	0.6	0.8	1	
$c^j(kT)$	-1	-1	-1	-1	-1	-1	-1	-1	-0.8	-0.6	-0.4	-0.2	0
	-0.8	-1	-1	-1	-1	-1	-1	-0.8	-0.6	-0.4	-0.2	0	0.2
	-0.6	-1	-1	-1	-1	-0.8	-0.6	-0.4	-0.2	0	0.2	0.4	0.6
	-0.4	-1	-1	-1	-0.8	-0.6	-0.4	-0.2	0	0.2	0.4	0.6	0.8
	-0.2	-1	-1	-0.8	-0.6	-0.4	-0.2	0	0.2	0.4	0.6	0.8	1
	0	-1	-0.8	-0.6	-0.4	-0.2	0	0.2	0.4	0.6	0.8	1	1
	0.2	-0.8	-0.6	-0.4	-0.2	0	0.2	0.4	0.6	0.8	1	1	1
	0.4	-0.6	-0.4	-0.2	0	0.2	0.4	0.6	0.8	1	1	1	1
	0.6	-0.4	-0.2	0	0.2	0.4	0.6	0.8	1	1	1	1	1
	0.8	-0.2	0	0.2	0.4	0.6	0.8	1	1	1	1	1	1
	1	0	0.2	0.4	0.6	0.8	1	1	1	1	1	1	1

The following figures show the simulation results with the altitude reference signal is $h_{ref}=50m$, and the reference signal corresponding to the velocity is $V_{ref}=5m/sec$.

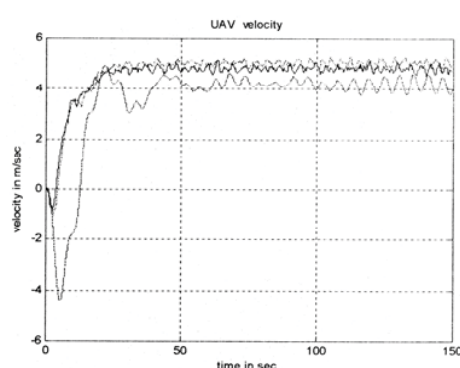
Table 2

H_2 -norm of the sensitivity function and H_∞ -norm of the complementary Sensitivity function

Plant		H_2	H_2	H_∞
$V_n=30$ [m/s]	nominal	0.2901	1.1725	0.0021
$V_{p1}=25$ [m/s]	Perturbed 1	0.7033	1.1725	0.0021
$V_{p2}=35$ [m/s]	Perturbed 2	0.3117	1.3749	0.0033



a.



b.

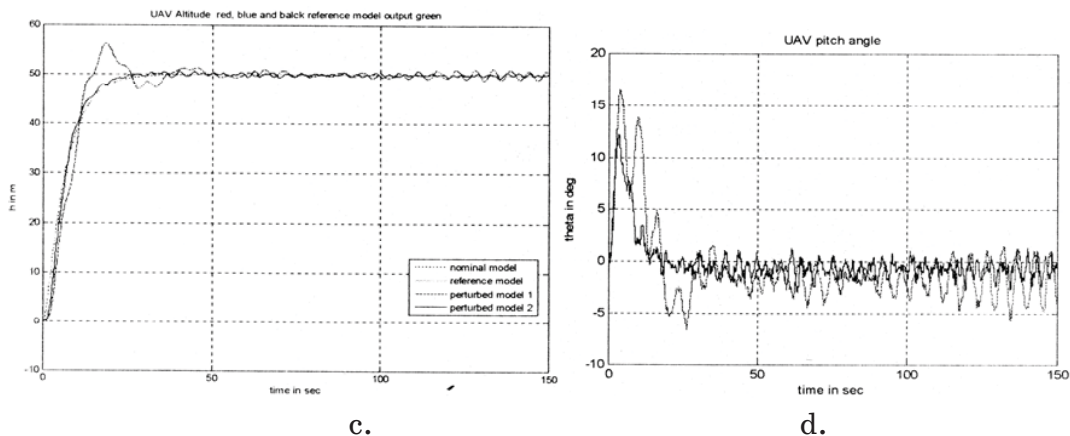


Figure 3 – Simulation results of Aerosonde longitudinal channel.

- a.velocity of UAV nominal and perturbed models;
- b.angle of attack of UAV nominal and perturbed models;
- c.pitch angle of UAV nominal and perturbed models;
- d.altitude of UAV nominal and perturbed models.

In the next table the adjusted rule base is given after simulation for the nominal model, for the sake of brevity the rule base for the first and the second perturbed model are not shown.

The entries of the rule base changed after the adaptation procedure are shown inside the bold rectangular.

Table 3

$U^{i,j}(kT)$	$e^i(kT)$											
		-1	-0.8	-0.6	-0.4	-0.2	0	0.2	0.4	0.6	0.8	1
$c^j(kT)$	-1	-1	-1	-1	-1	-1	-1	-0.8	-0.6	-0.4	-0.2	0
	-0.8	-1	-1	-1	-1	-1	-0.8	-0.6	-0.4	-0.2	0	0.2
	-0.6	-1	-1	-1	-1	-0.8	-0.6	-0.4	-0.2	0	0.2	0.4
	-0.4	-1	-1	-1	-0.8	-0.6	-0.4	-0.2	0	0.2	0.4	0.6
	-0.2	-1	-1	-0.8	-0.6	-0.467	-0.222	0.047	0.2	0.4	0.6	0.8
	0	-1	-0.8	-0.6	-0.4	-0.34	-0.0027	0.33	0.4	0.6	0.8	1
	0.2	-0.8	-0.6	-0.4	-0.2	-0.65	0.218	0.483	0.6	0.8	1	1
	0.4	-0.6	-0.4	-0.2	0	0.2	0.4	0.6	0.8	1	1	1
	0.6	-0.4	-0.2	0	0.2	0.4	0.6	0.8	1	1	1	1
	0.8	-0.2	0	0.2	0.4	0.6	0.8	1	1	1	1	1
	1	0	0.2	0.4	0.6	0.8	1	1	1	1	1	1

Conclusion

The purpose of the paper has been to design robust autopilot using combination of crisp control with hard computing and fuzzy control with soft computing. Procedure of robust H_2/H_∞ optimization has been used to achieve the trade-off between the robustness and performances of the system with crisp structure for inner-loop; the table 2 shows the efficiency of the procedure. The effectiveness of the proposed control scheme has been tested by computer simulation; the figures show that the flight requirement was respected for the nominal as well as for the perturbed models. The maximum angles deflections are all respected – $3 < \alpha < 3$, $-4 < \theta < 16$, and the altitude h is held at the reference signal ($50m$) as shown in the last figure. The velocity reference signal ($5m/sec$) is also tracked and is given in the first figure. All these deflections satisfy the specifications for this UAV.

REFERENCES

1. Robust Flight Control. A Design Challenge. J.-F. Magni, S. Bernani, J. Terlouw eds. Springer, London, 1997, 649 p.
2. Aerosim Blockset, www.u-dynamics.com/
3. Srinivasan K. Control System Design Using State Space Methods. In the book "Instrumentation, Systems, Controls, and Mems. Mechanical Engineers Handbook" edited by M. Kutz, the 3rd edition. John Wiley & Sons Inc., 2006, p.p.757-788.
4. Geromel G.C., De Souza C.C., Skelton R.E. Static Output Feedback Controllers: Stability and Convexity // IEEE Transactions on Automatic Control, Vol.43, № 1, January, 1998, pp. 120-125.
5. McLean D. Automatic Flight Control Systems. Prentice Hall Inc., Englewood Cliffs, 1990, 593 p.
6. Tunik A.A., Abramovich E.A. Parametric Robust Optimization of Digital Flight Control Systems // Proceedings of the National Aviation University, №2, 2003, pp.31-37.
7. Tunik A. A., Galaguz T. A. Robust Stabilization and Nominal Performance of the Flight Control System for Small UAV // Applied and Computational Mathematics, Vol. 3, №1, 2004, pp. 34 - 45.
8. Schoemig E., Sznaier M. Mixed H_2/H_∞ Control of Multi-model Plants. Journal of Guidance, Control and Dynamics, No.3, May-June, 1995, pp. 525-531.

9. Квакуернаак Х., Сиван Р. Линейные оптимальные системы управления. «Мир», М., 1977, 653 с.
10. Ackermann J. Parameter Space Design of Robust Control Systems, IEEE Transaction of Automatic Control, Vol. AC-25, № 6, December 1980, pp. 1058-1072.
11. Doyle J. C, Glover K., Khargonekar P. P., Francis B.A. State Space Solution to Standard H_2 and H -infinity Control Problems, IEEE Transaction of Automatic Control, Vol. 34, № 8, August 1982, pp.831-847.
12. Соколов Н. И., Рутковский В. Ю., Судзиловский Н. Б. Адаптивные системы автоматического управления летательными аппаратами.- М.: Машиностроение, 1988.-207с.
13. Гостев В.И. Синтез нечетких систем автоматического управления. 3-е издание, исправленное и дополненное.- К.: «Радиоаматор» , 2005.- 708с.
14. Passino, K.M., Yurkovich, S. Fuzzy Control. Addison-Wesley.- Menlo Park, Reading, Harlow, Berkley, Sidney, Bonn, Amsterdam, 1998. - 502 pages.
15. Piegat, A. Fuzzy Modeling and Control, Heidelberg, New York: Physic-Verl..-2001.-728p.
16. Kwakernaak, H. Robust Control and H_∞ - Optimization- Tutorial Paper. System and Control Group. Department of Applied Mathematics, University of Twente, September 1991, pp.255-273.